

RESEARCH ARTICLE

Computational Approach to the Discovery of Phytochemical Molecules with Therapeutic Potential Targets to the PKCZ protein

Poliany G. Freitas^{1,*}, Thiago C. Elias¹, Icaro A. Pinto¹, Luciano T. Costa^{1,2}, Paulo V.S.D. de Carvalho³, Daniel de Q. Omote⁴, Ihosvany Camps¹, Tati Ishikawa⁵, Helen A. Arcuri⁶, Susana Vinga⁷, Arlindo L. Oliveira⁸, Walter F.A. Junior⁹ and Nelson J.F. da Silveira^{1,8}

¹Laboratory of Molecular Modeling and Computer Simulations-MolMod-CS, Institute of Exact Sciences, Federal University of Alfenas, Alfenas, Brazil; ²Laboratory of Molecular Modeling and Computer Simulation-MolMod-CS, Institute of Chemistry, Federal Fluminense University, Niterói, Rio de Janeiro, Brazil; ³Laboratory of Cellular and Molecular Genetics, Federal University of Minas Gerais Brazil and Department of Mathematics and Computer Science, University Southern of Denmark, Odense, Denmark; ⁴Sleep Laboratory, Heart Institute (InCor), Faculty of Medicine, University of São Paulo, São Paulo, Brazil; ⁵Department of Medicine and Food, Faculty of Pharmaceutical Sciences, Federal University of Alfenas, Alfenas, Brazil; ⁶Center of the Study of Social Insects, Department of Biology, Institute of Biosciences of Rio Claro, São Paulo State University, Rio Claro, SP, São Paulo, Brazil; ⁷IDMEC, Higher Technical Institute, University of Lisboa, Lisboa, Portugal; ⁸INESC-ID / Higher Technical Institute, Lisboa, Portugal; ⁹Laboratory of Computational Systems Biology, Faculty of Biosciences, Pontifical Catholic University of Rio Grande do Sul (PUCRS), Porto Alegre, Brazil

ARTICLE HISTORY

Received: June 13, 2017
Revised: July 31, 2017
Accepted: August 01, 2017

DOI:
10.2174/1570180814666170810115134

Abstract: Background: Head and neck squamous cell carcinoma (HNSCC) is one of the most common malignancies in humans and the average 5-year survival rate is one of the lowest among aggressive cancers. Protein kinase C zeta (PKCZ) is highly expressed in head and neck tumors, and the inhibition of PKCZ reduces MAPK activation in five of seven head and neck tumors cell lines. Considering the world-wide HNSCC problems, there is an urgent need to develop new drugs to treat this disease, that present low toxicity, effective results and that are relatively inexpensive.

Method: A unified approach involving homology modeling, docking and molecular dynamics simulations studies on PKCZ are presented. The *in silico* study on this enzyme was undertaken using 10 compounds from latex of *Euphorbia tirucalli* L. (aveloz).

Results: The binding free energies highlight that the main contribution in energetic terms for the compounds-PKCZ interactions is based on van der Waals. The per-residue decomposition free energy from the PKCZ revealed that the compounds binding were favorably stabilized by residues Glu300, Ileu383 and Asp394. Based on the docking, Xscore and molecular dynamics results, euphol, β -sitosterol and taraxasterol were confirmed as the promising lead compounds.

Conclusion: The present study should therefore play a guiding role in the experimental design and development of euphol, β -sitosterol and taraxasterol as anticancer agents in head and neck tumors. They are potential lead compounds, better than other ligands based on the best values of docking and MM-PBSA energy.

Keywords: HNSCC, PKCZ, molecular marker, euphorbia tirucalli, homology modeling, molecular docking, molecular dynamics.

1. INTRODUCTION

Head and neck squamous cell carcinoma (HNSCC) develops in the oral cavity and is the sixth leading cancer by

incidence worldwide. This year, globally, 600,000 new cases of head and neck cancer are likely to occur and of these, 40-50% with HNSCC will only survive for 5 years [1]. According to the World Cancer Report of 2014, adding up pharyngeal, oral and laryngeal cancers in both sexes combined, 686,000 new cases were estimated for the year of 2012 with 375,000 estimated deaths for the same year. A decline in incidence can be seen since the 1990s for some countries such as India, China, USA, and Australia. However, conversely, increasing trends in incidence are being shown in

*Address correspondence to this author at the Laboratory of Molecular Modeling and Computer Simulation-MolMod-CS, Institute of Exact Sciences, Federal University of Alfenas – UNIFAL-MG, Gabriel Monteiro da Silva 700, Centro, 37130-001, Alfenas, Brazil; Tel/Fax: +55 35 3701-9602; E-mail: poliany.santos@gmail.com

countries such as Denmark and Japan [2]. In Brazil alone, 15,490 new oral cancer cases are estimated for the year of 2016, and this cancer was responsible for 5,401 deaths in 2013. In regard to laryngeal cancer, 4,141 deaths were recorded in Brazil in the year of 2013 and 7,350 new cases are expected for 2016, 6,360 of those affecting men [3]. The development of head and neck malignancies is strongly associated with certain risk factors such as tobacco use, alcohol consumption and infection with high-risk types of human papilloma virus (HPV) [4, 5].

The diagnosed cases of this disease are often at an advanced stage, with a significant burden of lymph node involvement. Treatment of these patients involves assessment by a multidisciplinary team with the coordination of surgery, chemotherapy and radiation therapy. In most cases, combination therapy is used [6]. However, nonsurgical treatment has a low response rate and high side effects. Despite advances in research and treatment, clinical outcomes and overall survival rates for HNSCC have not been improved substantially over the past decades, with the overall 5 years survival rate under 50%. However, there is ongoing research on potential alternatives and less toxic therapies for cancer of the head and neck, seeking to achieve a more favorable clinical outcome by reducing treatment morbidity [7]. Recent research on differentially expressed genes, biological functions and potential involvement in HNSCC has shown that a protein kinase C (PKC) zeta type participates in the biological process of regulation of cell growth [5]. PKC has been implicated as a mediator of epidermal growth factor receptor (EGFR) signaling in certain cell types. EGFR is top-up expressed in HNSCC and plays a key role in tumor progression and PKCZ is necessary for the proliferation and viability of tumor cells [8]. The inhibition of PKCZ reduces MAPK activation in normal human adult epidermal keratinocytes in five out of seven head and neck tumor cell lines. Furthermore, squamous cell carcinomas of the head and neck cell proliferation and viability are reduced by the inhibition of PKCZ [8, 9]. Therefore, PKCZ is a potential prognostic biomarker for target therapy of such tumors and its inhibition potentiates the action of other growth inhibitors in HNSCC. The objective of this work is to study the interaction mechanisms of molecules identified in the latex of *Euphorbia tirucalli* L. with PKCZ.

E. tirucalli (Euphorbiaceae), popularly known as “aveloz”, is a succulent shrub native from Africa and widely employed in Brazilian traditional medicine [10]. The bark/latex of *E. tirucalli* shows pharmacological activities such as antibacterial, molluscicidal, antiherpetic and antimutagenic [11]. In northeastern Brazil, the latex of *E. tirucalli* is used as a folk medicine against syphilis and intestinal parasites, on the treatment of asthma, earache, cough, rheumatism, cancer and skin tumors [12]. Ethnobotanical studies in Brazil show that among a total of 84 medicinal plant species that were reported in the ethnobotanical/ethnopharmacological literature as being used for the treatment or prevention of cancer and tumors, the most represented botanic family was Euphorbiaceae, *E. tirucalli* being one of the most cited species [13]. Furthermore, studies proposed to search for the antitumoral activity of the *E. tirucalli* on the morphology and progression of the tumor cells have shown that cell proliferation was

decreased [14-16]. Chemically latex comprises mostly terpenes and sterols, including euphol, α -euphorbol, cycloeuphor-denol, euphorginol, tiglane (phorbol esters), ingenane (ingenol esters), lupeol, α -amyirin, lanosterol, cycloartenol, taraxasterol, tirucallol, cyclotirucanenol and tirucallicine [17, 18]. The species is also reported to possess hentriacontane, β -sitosterol, succinic acid, citric acid, ellagic acid, 3,3'-di-*O*-methylellagic acid, gallic acid, catechin, myricetin, tellimagrandin II, geraniin, euphorbin A, tirucallin A and B, prostratin A, euphorbin F, pedunculagin, putranjivain A and B, corilagin, casuariin, 5-desgalloylstarchyurin and 3,3,4-tri-*O*-methyl-4-*O*-rutosyl ellagic acid [19-25].

Currently, scientists are focusing on designing and discovering potential inhibitors against cancer-related proteins that play a critical role in the development of a variety of tumors. Future research breakthroughs with the aid of computer-aided molecular design and chemo-bioinformatics will bring new hope, but also create a new class of anticancer drugs that will help millions of cancer patients. Thus, designed drugs are expected to have high affinity to the novel targets, inhibit the proliferation and differentiation of tumor cells and speed up their death. *In silico* Lipinski's rule predictions, database screening and molecular modeling studies are useful tools for investigating biological receptors and bioactive ligands. The above techniques can be used to investigate and report a new ligand for a candidate target protein. A combination of more structures, advances in homology modeling, better docking and scoring tools, molecular dynamics simulations, fragment-based methods, and advances in virtual screening have been fundamental in this progress [26, 27].

Molecular docking is a method which identifies the preferred orientation of one molecule and the affinity, when bound to another, to form a stable protein-ligand complex. Knowledge of preferred orientation can in turn be used to predict the binding affinity between two molecules using, for example, scoring functions. Molecular docking algorithms fit molecules together in complementary fashions. This technique has attracted increasing attention from many researchers as a way to predict the geometries of complex biomolecules and their affinities [27-29]. XScore is a score function used to compute energy interaction between protein-ligand complexes and may be used to rescore and/or confirm binding affinities obtained in virtual screening procedures [30]. Its final value is determined by average of three independent functions that is composed of five terms accounting for van der Waals interactions, hydrogen bonding, deformation effect, hydrophobic effect, and translational and rotational entropy loss effect. Another tool for molecular modeling studies is the molecular dynamics (MD) simulation that is used to study the interaction and movement of molecules. The MD and molecular mechanics Poisson-Boltzmann surface area (MM-PBSA) methods when combined to rescore the docked complexes have been widely used for the choice of the best ligand [31].

Among the substances present in the latex, 10 molecules were selected for *in silico* discovering of better interacting molecules with PKCZ. This paper aims to provide a model of the structure of tridimensional PKCZ by molecular modeling and find a drug target compound as a leader from the

molecules present in the latex of *E. tirucalli* by docking and molecular dynamics simulations with the enzyme PKCZ. The present study has been carried out to test the efficiency of the naturally occurring plant compounds against the molecular marker PKCZ expressed in head and neck tumors.

2. MATERIALS AND METHOD

2.1. Homology Modeling

We made a model structure of PKCZ using the MODELLER9.15 program [32]. Initially, the primary sequence of the target was obtained from Uniprot [33] (UniProtKB: Q05513). This sequence consists of 592 residues, in which residues Thr410 and Thr560 are phosphorylated. The sequence was submitted to a BLAST run for template selection using Protein Data Bank (PDB) [34] as database and the PSI-BLAST algorithm [35]. Among the potential returned templates, a human PKC ϵ kinase structure (PDBcode: 3A8W) [36] was selected, due to its 2.10 Å resolution and 84.43% similarity with the target. Sequence alignment was carried out using ClustalO web service [37] and the alignment was converted to PIR format. In the modeling, the two modified phosphorylated threonines were transferred from template to model, using “env.io.hetatm = true” command in the program script. 60 models were generated and the best model was chosen by PROCHECK analysis [38].

2.2. Molecular Docking

The inhibitor midostaurin was used as a control drug in molecular docking. Ten natural products were selected from *E. tirucalli* for docking studies, namely: ellagic acid, kaempferol, 3,3'-di-*O*-methylellagic acid, taraxasterol, β -sitosterol, euphol, citric acid, hentriacontane, malic acid and succinic acid. Their structures were obtained from PubChem [39] in sdf format, converted to mol2 format using openbabel software [40], and prepared using prepare_ligand4.py script from MGLTools programs suite [41]. The selected PKCZ model was prepared using prepare_receptor4.py script. Docking running was performed by AutoDock Vina program [42]. A related PKC ϵ structure (PDBcode: 3A8X, resolution: 2.10 Å) [36] has a co-crystallized ATP in site formed by residues Ile251, Gly252, Gly254, Ser255, Tyr256, Ala257, Val259, Lys274, Ile323, Glu324, Val326, Asp387 and Phe543, corresponding to residues Ile258, Gly259, Gly261, Ser262, Tyr263, Ala264, Val266, Lys281, Ile330, Glu331, Val333, Asp394 and Phe552 in the model, thus, these residues were used for search space identification, that was centered at x-y-z point 21.723, -1.863, -37.296, with box dimension of 20.562 X 26.710 X 19.912 Å. Addition, we computed binding energy using Xscore program [30].

2.3. Molecular Dynamics

The PKCZ-compound complexes of the best docking poses were placed in a cubic periodic box and solvated by 24822 water molecules using a transferable intermolecular potential 3P (TIP3P) model for water molecules [43]. The AMBER99sb force field was used for PKCZ model. Force field parameters for the small molecules were obtained by generalized amber force field (GAFF) [44]. Amber topologies for the compounds were converted to GROMACS for-

mat using acpype [45]. The system was neutralized and ionic strength (0.15 mol L^{-1}) of the medium was adjusted by adding Na^+ and Cl^- . The molecular dynamics simulations were performed using GROMACS software package [46-48] keeping constant the number of particles, pressure, and temperature (NpT ensemble) at 300 K and 1.0 bar using the velocity-rescaling [49] and Parrinello-Rahman [50] methods for temperature and pressure control with 0.1 ps and 2.0 ps time coupling, respectively. Equilibration periods were 1.0 ns, and productions runs were 10 ns. A cutoff distance 1.2 nm has been used for calculations of Lennard-Jones interaction and particle mesh Ewald (PME)[51] was used for the long-range electrostatic interactions. The bond lengths of hydrogen atoms were controlled with the LINCS [52] algorithm, and the SETTLE [53] algorithm was used to constrain the geometry of the water molecules.

Binding free energy estimation for PKCZ-compound complexes based on molecular mechanics/Poisson-Boltzmann solvent-accessible surface area (MM-PBSA) [31] was calculated from the g_mmpbsa tool implemented in the subroutine of GROMACS and APBS [54]. The binding free energy was estimated from 100 snapshots extracted every 10 ps of the DM trajectories which do not include the term entropy. The LigPlot⁺ [55] was used to evaluate the interactions complexes.

2.4. Lipinski's rule of five analysis

The Lipinski's rule of five was analyzed for all ligands considered for this study by calculating the corresponding ADME properties using FAF-Drugs3 web server [56]. Lipinski's rule of five was initially developed to be applied only to absorption by passive diffusion of compounds through cell membranes. Due to their simplicity, it is widely used to evaluate the overall drug-likeness.

3. RESULTS AND DISCUSSION

3.1. PKCZ model Overview

The PKCZ model was constructed by homology modeling based on the PKC ϵ template using MODELLER program, through the 84.43% similarity with the target. The target residues 1-243 and 585-592 did not have equivalents in the template structure, therefore we did not consider them in the building model. Primary sequence alignment between the target and template is shown in Fig. (1), where the active site residues are surrounded by red squares. Active site residues are totally conserved in both sequences. Among 60 generated models, the model 34 was chosen for docking and molecular dynamics studies. In the Ramachandran plot, the model 34 exhibited 94.3% of the residues in the most favorable regions, 5.0% in the additional allowed regions, 0.7% in the generously allowed regions and 0.0% in the disallowed region. 3D alignment between target and template shows an RMSD = 0.403 Å (calculated by pymol software [57]) (Fig. 2) has come under the expected range of ≤ 2.0 Å [58].

3.2. Molecular Docking

The molecular docking results are shown in Tables 1 and 2D ligand structures in Fig. (3). Among natural products,


```

3A8X      MDPLGLQDFDLIRVIGRGSYAKMLLVRLKKTDRITYAMKVVKKELVNDDDEDIDWVQTEKHV
PKCZ      SQGLGLQDFDLIRVIGRGSYAKMLLVRLKKNQIYAMKVVKKELVHDDDEDIDWVQTEKHV
          : ***** : ***** : ***** : ***** : ***** :
          :

3A8X      FEQASNHPFLVGLHSCFQTESRLFFVTEYMNGGDLMFHMQRQRKLPEEHARFYSAEISLA
PKCZ      FEQASSNPFLVGLHSCFQTTSRFLVTEYMNGGDLMFHMQRQRKLPEEHARFYAAEICIA
          ***** : ***** : ***** : ***** : ***** :
          :

3A8X      LNYLHERGIIYRDLKLDNVLLDSEGHIKLTDYGMCKEGLRPGDTTSTFCGTPNYIAPEIL
PKCZ      LNFLHERGIIYRDLKLDNVLLDADGHIKLTDYGMCKEGLRPGDTTSTFCGTPNYIAPEIL
          ** : ***** : ***** : ***** : ***** :
          :

3A8X      RGEDYGFSDVWALGVLMFEMMAGRSPFDIVGS-----TEDYLFQVILEKQIRIPRSLSV
PKCZ      RGEYGFSDVWALGVLMFEMMAGRSPFDIITDNPDMNTEDYLFQVILEKPIRIPRFLSV
          *** : ***** : ***** : ***** : ***** :
          :

3A8X      KAASVLKSFLNKDPKERLGCHPQTGFADIQGHPPFRNVWDMMEQQVPPFKPNISGEF
PKCZ      KASHVLKGFNLKDPKERLGRPQTGFSDIKSHAFFRSIDWDLLEKKQALPPFQPQITDDY
          ** : *** : ***** : ***** : ***** : ***** : ***** :
          :

3A8X      GLDNFDSQFTNEPVQLTPDDDDIVRKIDQSEFEGFEYINPL
PKCZ      GLDNFDTQFTSEPVQLTPDDEDAIKRIDQSEFEGFEYINPL
          ***** : ***** : ***** : ***** : ***** :
          :

```

Fig. (1). Sequence alignment between human PKC α from PDB structure 3A8X and human PKC ζ . In the alignment, the PKC ζ sequence ranges from residue 244 to residue 584. Active site residues in both sequences are surrounded by a red square. Sequence alignment performed by ClustalO web service [37].

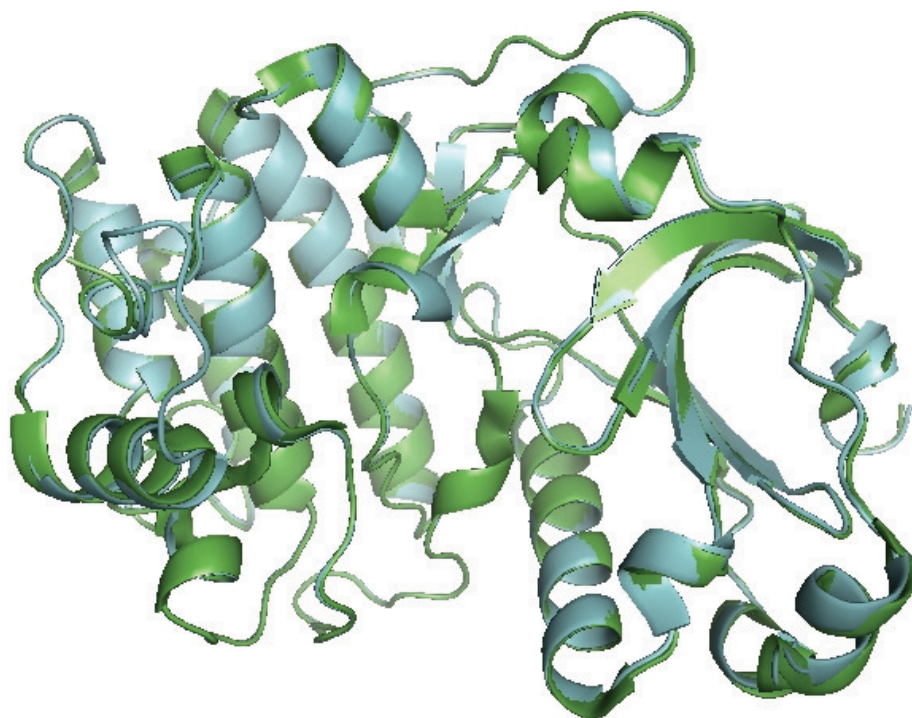


Fig. (2). Superposition between PKC ζ model and 3A8X pdb template. Blue: PKC ζ model, green: 3A8X PDB structure. Rendered by pymol program [57].

Table 1. Binding free energy (kcal mol⁻¹) results of PKCZ model with *Euphorbia tirucalli* natural products obtained by AutoDock Vina program, Xscore and MMPBSA-molecular dynamics. LogP was obtained by obprop program [40].

Compounds	Formula	$\Delta G_{\text{Vina Score}}$	ΔG_{Xscore}	$\Delta G_{\text{MM-PBSA/molecular dynamics}}$	LogP
Taraxasterol	C ₃₀ H ₅₀ O	-10.7	-10.97	-33.83	8.0248
Euphol	C ₃₀ H ₅₀ O	-9.5	-10.39	-37.00	8.4791
β -Sitosterol	C ₂₉ H ₅₀ O	-8.9	-9.94	-33.19	8.0248
Ellagic Acid	C ₁₄ H ₆ O ₈	-8.4	-7.80	-19.16	1.3128
3,3'-di-O-methylellagic Acid	C ₁₆ H ₁₀ O ₈	-8.3	-7.77	-22.51	1.9188
Kaempferol	C ₁₅ H ₁₀ O ₆	-8.2	-8.06	-22.71	2.2824
Hentriacontane	C ₃₁ H ₆₄	-5.4	-8.21	-14.98	12.3391
Citric Acid	C ₆ H ₈ O ₇	-4.9	-6.23	-12.14	-1.2485
Malic Acid	C ₄ H ₆ O ₅	-4.1	-5.82	-12.66	-1.0934
Succinic Acid	C ₄ H ₆ O ₄	-4.0	-5.85	-1.96	-0.0642
Midostaurin	C ₃₅ H ₃₀ N ₄ O ₄	-10.7	10.85	----	-5.89

Table 2. Lipinski's values of phyto-compounds.

Compounds	MW	QPlog Po/w	HB Donor	HB Acceptor	Lipinski Violations (max.4)
Taraxasterol	426.724	7.075	1	1	1
Euphol	384.644	7.111	1	1	1
β -sitosterol	414.713	7.435	1	1	1
Ellagic acid	302.197	-1.391	4	8	0
3,3'-di-O-methylellagic acid	330.250	0.002	2	8	0
Kaempferol	286.236	1.630	4	6	0
Hentriacontane	436.847	16.318	0	0	1
Citric acid	192.125	-0.261	4	7	0
Malic acid	134.088	-0.450	3	5	0
Succinic acid	118.089	-0.579	2	4	1

taraxasterol, euphol and β -sitosterol exhibit the best binding energy for VinaScore. The control drug (midostaurin) has a binding energy of -10.7 kcal.mol⁻¹ being the same as of taraxasterol. In this way, we can suggest that these three natural products have good interaction with PKCZ active site. In order to validate molecular docking, the binding energy was also calculated by Xscore confirming that taraxasterol, euphol and β -sitosterol exhibit better interaction with PKCZ. The most hydrophilic ligands demonstrate a lower binding energy, accordingly with the hydrophobic characteristic of PKCZ active site. LogP values were calculated by obprop program of openbabel tools [40]. Binding energy and logP roughly correlated, the three ligands with the best binding energy (taraxasterol, euphol and β -sitosterol) had higher logP values, while the three ligands with lower binding en-

ergy (citric acid, malic acid and succinic acid) had lower logP values. An exception is hentriacontane, that has the highest logP value, but low binding energy, likely due its long opened chain with 31 carbon atoms, which could not fit well into the active site. Ligplot graphics [55] are shown for taraxasterol-, euphol- and β -sitosterol-PKCZ complexes (Fig. 4). Interaction between PKCZ and taraxasterol was mediated by hydrophobic contacts, while interaction with euphol showed H-bonding with Glu331 and Val333 residues, and β -sitosterol showed H-bonding with Glu331.

3.3. Molecular Dynamics

Molecular dynamics simulations were performed to refine the complexes obtained by molecular docking, to verify the stability and to free energy rescoring all the structures by

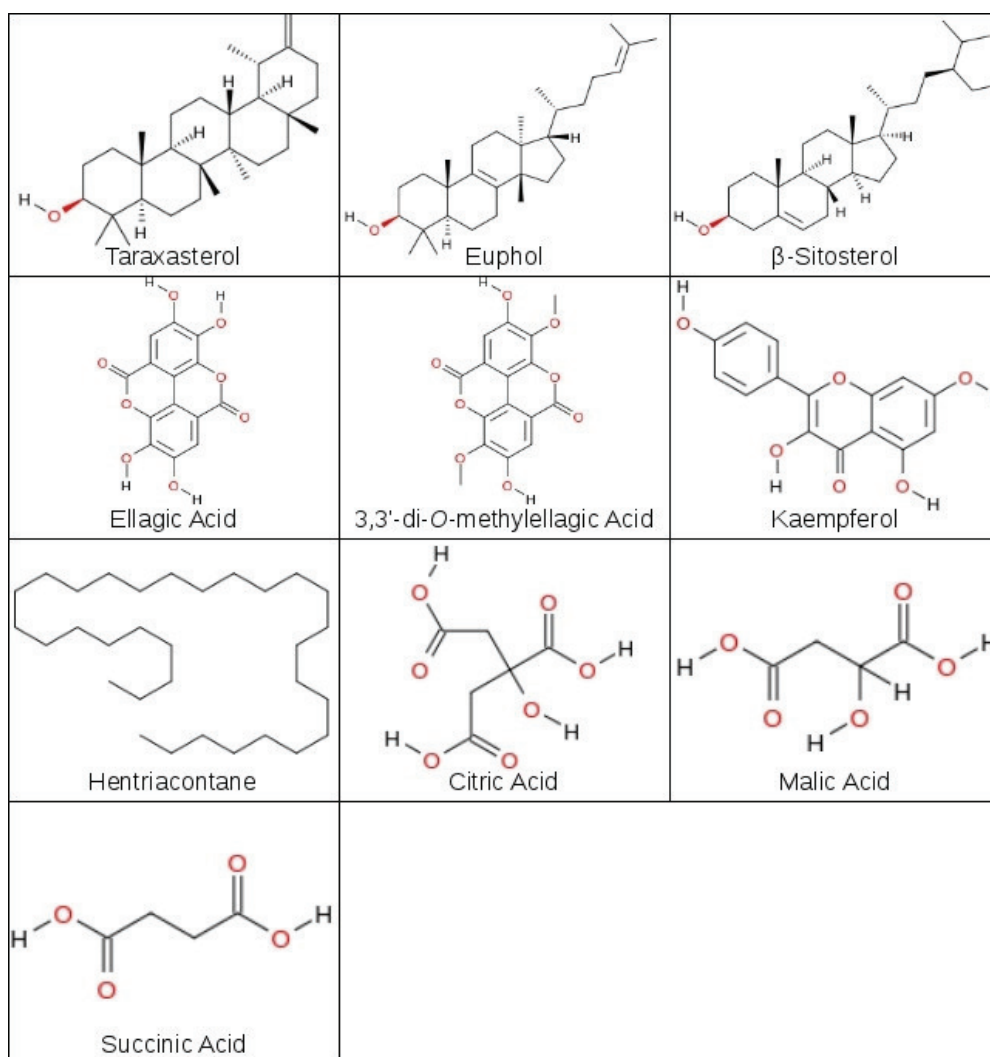


Fig. (3). Ligands selected from *Euphorbia tirucalli* for docking and molecular dynamics study.

the molecular mechanics/Poisson–Boltzmann solvent accessible surface area (MM-PBSA) method [31]. The stability of the complexes can be verified by the calculation of root mean square deviation (RMSD) of the structure, which determines the deviation between the positions of the starting atoms in relation to the trajectory of MD. Fig. (5a) shows the results obtained from RMSD for the three best complexes. Observing the last 6 ns, the protein stabilizes reaching average RMSD values of 0.255 ± 0.013 , 0.239 ± 0.018 and 0.246 ± 0.019 nm when complexed with euphol, β -sitosterol and taraxasterol, respectively, suggesting that the complexes were similarly stable.

The radius of gyration (Rg) confers the hydrodynamic capacity of the protein, and it can verify how compact or not the protein becomes in the complex. Fig. (5b) shows that the Rg for the complex with euphol presents smaller fluctuations, being more stable in relation to others. However, the complexes with β -sitosterol and taraxasterol show large fluctuations up to 4 ns reaching values 2.189 and 2.193 nm, respectively, and after 4 ns, the fluctuations decreased and became stable. Thus, the average Rg values of the last 6 ns

were 2.137 ± 0.009 , 2.141 ± 0.008 and 2.161 ± 0.011 nm for the complexes with euphol, β -sitosterol and taraxasterol, respectively, suggesting that the protein is more compact with a lower hydrodynamic radius when complexed with euphol. Root mean square fluctuation (RMSF) with respect to each residue was calculated (Fig. (5c)). The fluctuation was highest in the loop region from 450 to 480 amino acid residues outside the binding site. These results are in agreement with the radius of gyration, since the mobility of the residues is higher for taraxasterol and lower for the euphol. In sum, these results suggest that the euphol-PKCZ complex is the most stable over time of simulation.

Molecular mechanics Poisson-Boltzmann surface area (MM-PBSA) method has been used to estimate binding free energies for the study of biomolecular interactions as well as for scoring function in drug design [31]. The binding free energy of the 10 complexes was calculated by the average of 100 poses throughout the MD simulations (Table 1). The binding free energy showed the best ligands for PKCZ, euphol (-37.00 kcal mol⁻¹), β -sitosterol (-36.19 kcal mol⁻¹) and taraxasterol (-33.83 kcal mol⁻¹). This result corroborates with

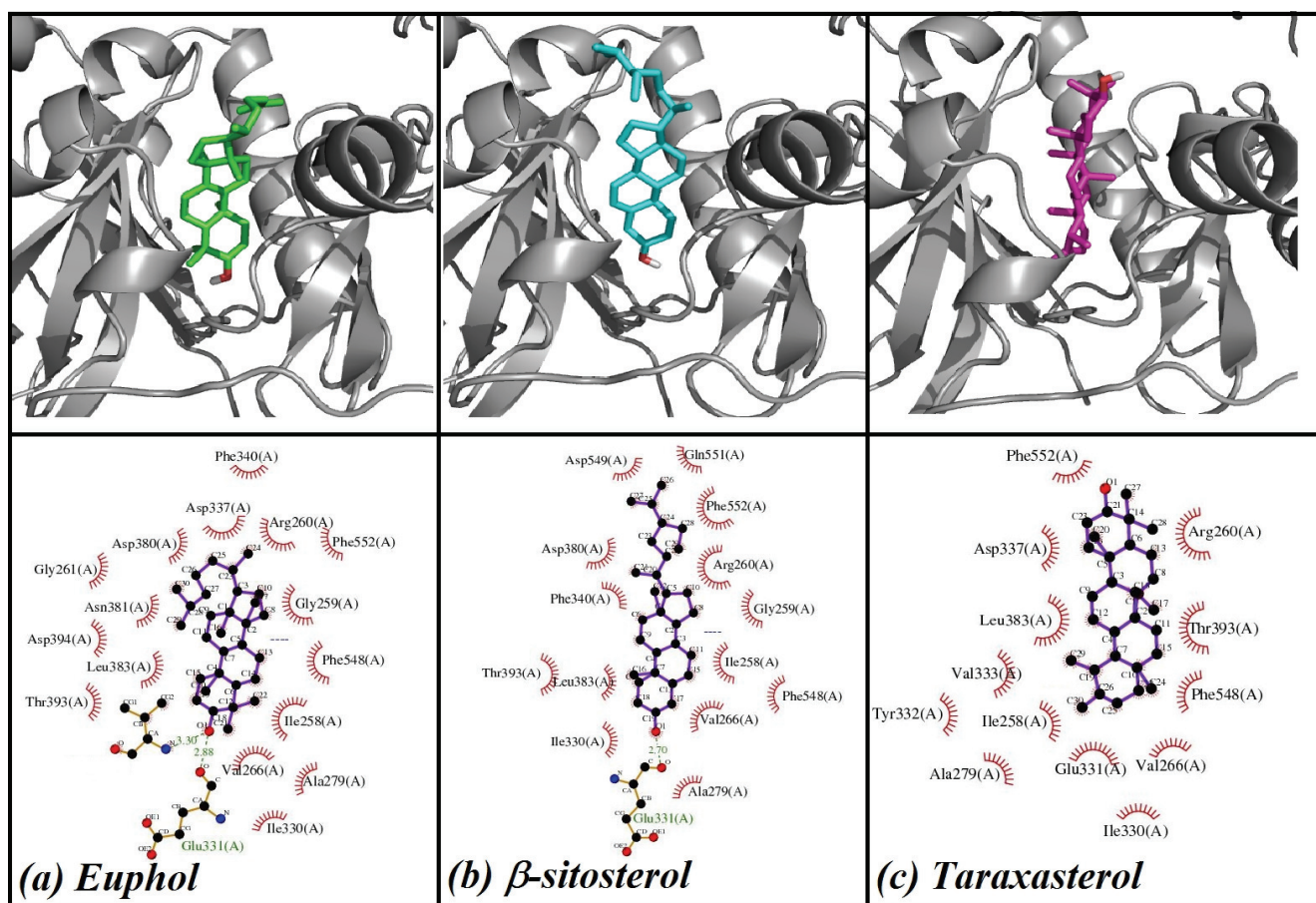


Fig. (4). Interaction of PKCZ with the best ligands obtained by molecular docking. The PKCZ is shown in gray color cartoon while the compounds are depicted by sticks. Green, cyan and magenta sticks represent euphol, β -sitosterol and taraxasterol, respectively. Thatched semi-circles indicate van der Waals contacts between hydrophobic protein residues and compounds. Hydrogen bonds are shown as green dashed lines.

the energy calculated by the docking and Xscore where these compounds also presented better binding energy. Among the energies that contribute to the interaction energy, van der Waals energy (-48.61 , -41.19 and -38.78 kcal mol $^{-1}$) has a larger contribution, followed by the solvent accessible surface area energy (-4.78 , -4.98 and 3.20 kcal mol $^{-1}$) and electrostatic energy (-4.21 , 4.19 and 1.09 kcal mol $^{-1}$), whereas the polar solvation energy (20.62 , 14.16 and 9.95 kcal mol $^{-1}$) does not present an effective contribution due to the positive values for the complexes euphol-, β -sitosterol- and taraxasterol-PKCZ, respectively. This is evidence that the energy governing the interaction force with the compounds is van der Waals. The energy decomposition analysis (Fig. 6) shows the main contributions from residues Glu300, Ile383 and Asp394 to three compounds with energy ≤ -1.5 kcal mol $^{-1}$. It is shown that Lys281 is in disfavor with the binding for three compounds. Fig. (7) shows interaction that occurs between PKCZ and the top three compounds calculated by ligplot from the final structure of the MD simulation. In all poses, van der Waals contacts were observed between hydrophobic protein residues and taraxasterol euphol and β -sitosterol; moreover, for euphol and β -sitosterol, which also include hydrogen bonding. It is noted that these bonds are conserved in both the docking and MD analyzes with residues Glu331,

Val333, which may also be associated with good stability of the complex beyond the hydrophobic interactions. However, it is observed that the residues with greater energy contribution (Fig. 6) make hydrophobic interaction, reaffirming that the van der wall energy is the force that governs the interaction with PKCZ.

The study shows that triterpenes euphol, taraxasterol and β -sitosterol bind the PKCZ with ATP-binding pocket revealed by three different methods, docking, Xscore and molecular dynamics. There are reports demonstrated by different experimental studies, where triterpenes present anti-inflammatory and anti-cancer activity. In addition, studies show that these molecules decrease the activity of enzyme kinases like PKC and Epidermal Growth Factor Receptor (EGFR) and also bind in the ATP-binding pocket [59-62]. Therefore, based on the results of stability and binding free energy performed by MD the best molecules present in the latex of *E. tirucalli* to binds PKCZ is euphol. However, it has been reported that this molecule reduces the activation of PKC α , PKC δ , and PKC ϵ ; the isozymes expressed in human [59]. In light of these evidences, these triterpenes can be used as a good prototype candidate in the development of new drugs for cancer treatment, as inhibitors proteins kinase

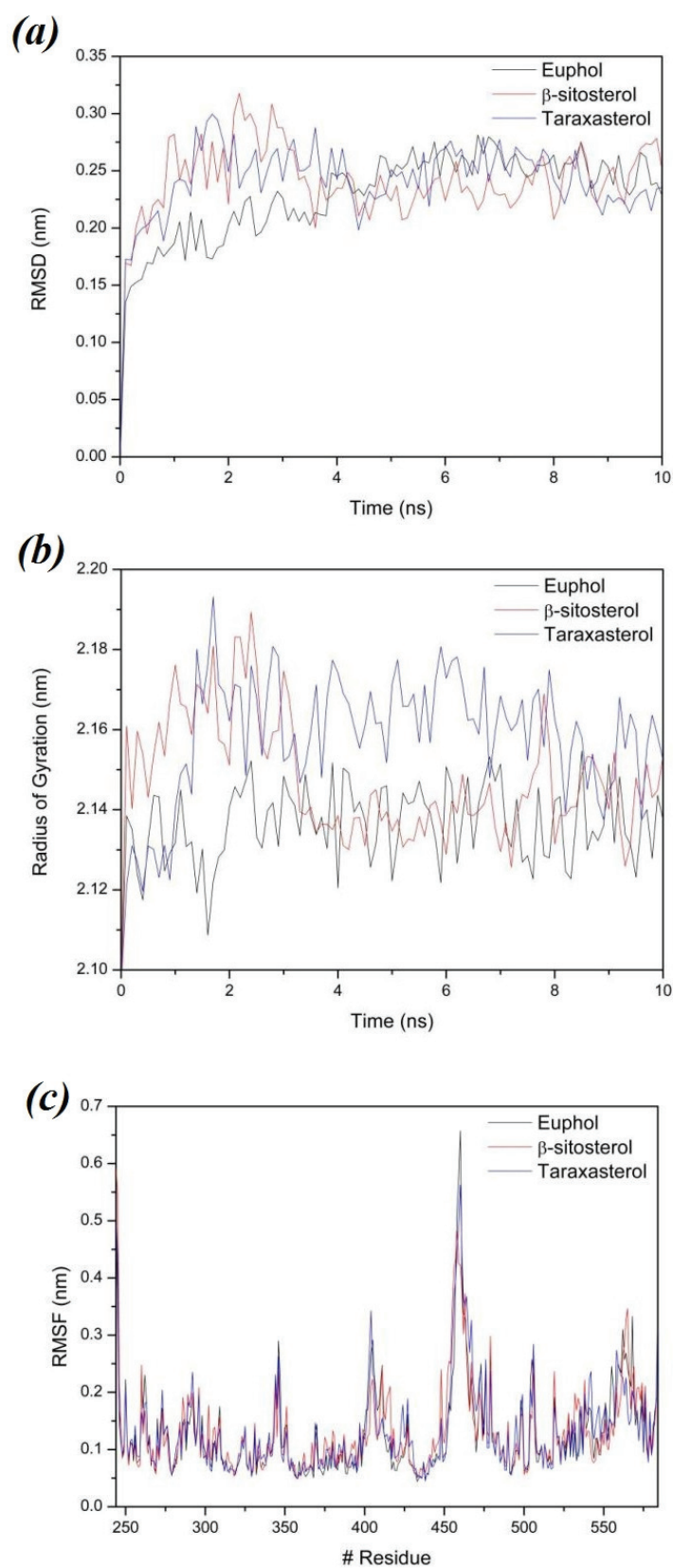


Fig. (5). The RMSD, radius of gyration and RMSF graph for three complex systems. (a) The RMSD profile for the C-alpha of PKCZ protein. (b) The radius of gyration of the systems. (c) RMSF of the systems.

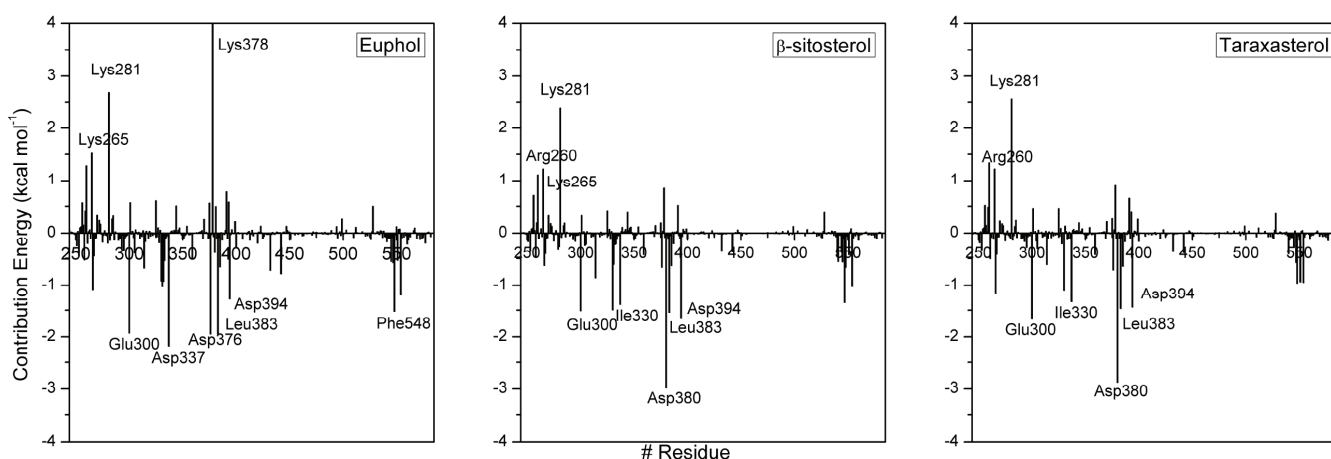


Fig. (6). Per-residue decomposition free energy of the PKCZ for the three complexes from simulations.

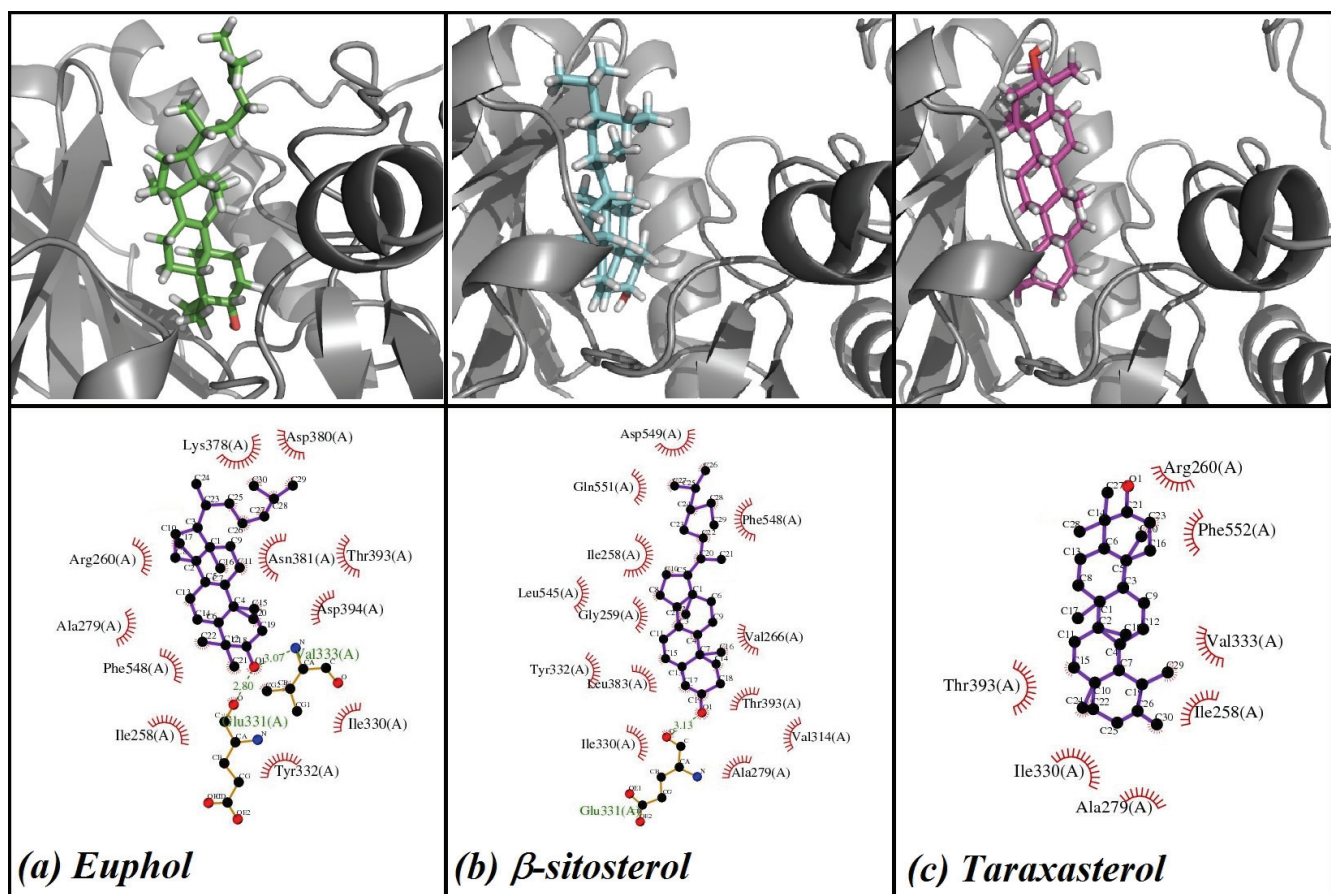


Fig. (7). The binding mode and schematic representation of the final structure of MD. The PKCZ is shown in gray color cartoon while the compounds are depicted by sticks. Green, cyan and magenta sticks represent euphol, β -sitosterol and taraxasterol, respectively. Thatched semi-circles indicate van der Waals contacts between hydrophobic protein residues and compounds. Hydrogen bonds are shown as green dashed lines.

C, although additional experiments are necessary to establish the potential efficacy of these triterpenes.

3.4. Lipinski's Rule

Lipinski's rule of five evaluates drug-likeness and determines whether the compound is pharmacologically active.

This filter is widely used for the development of new drugs. Table 2 shows the Lipinski's rule of five. Only five compounds were found to comply with the Lipinski's rule. Furthermore, five compounds violated only one Lipinski's rule and a drug to be rejected must present more than one violation of the following criteria (the rule-of-five (RO5)): molecular weight

≤ 500 ; calculated log P (LogP) ≤ 5 ; number of hydrogen bond donors (HBD) ≤ 5 ; number of hydrogen bond acceptors (HBA) ≤ 10] [63].

CONCLUSION

The PKCZ model generated can be used for docking and molecular dynamics studies. The developed model has shown good overall structural quality as confirmed using different validation tools. Thus, the present work forms the basis for further molecular modeling and biochemical studies on targeting the PKCZ enzyme for therapy. Our studies revealed euphol, β -sitosterol and taraxasterol as potent lead compounds, better than other compounds based on the best values of docking and MM-PBSA energy. In addition, the binding energy of the control drug was the same as that of taraxasterol, suggesting that the best ligands may have good interaction with the PKCZ active site. Among the energy contributions resulting from MM-PBSA binding free energies the van der Waals energetic term is the key compound-PKCZ interaction. In addition, these three complexes showed good stability over time of the MD simulations. However, based on the MD data, the best interaction of PKCZ is euphol, since MD considers the flexibility of both the protein and the ligand in the complex, resulting in a proper adjustment of the ligand at the binding site. Further, *in vitro* and *in vivo* analysis of the effects of euphol, β -sitosterol and taraxasterol will be necessary to accurately understand its molecular mechanism of action and pharmacological efficiency to conclusively state that they can be used as prototypes candidates in the development of new drugs for of HNSCC.

LIST OF ABBREVIATIONS

HNSCC	=	Head and neck squamous cell carcinoma
PKCZ	=	Protein kinase C zeta
MAPK	=	Mitogen-activated protein kinase
MM-PBSA	=	Molecular mechanics/Poisson-Boltzmann solvent-accessible surface area
HPV	=	Human papilloma virus
EGFR	=	Epidermal growth factor receptor
MD	=	Molecular dynamics
RMSD	=	Root mean square deviation
Rg	=	Radius of gyration
RMSF	=	Root mean square fluctuation
ADME	=	Absorption, distribution, metabolism, and excretion

ETHICS APPROVAL AND CONSENT TO PARTICIPATE

Not applicable.

HUMAN AND ANIMAL RIGHTS

No Animals/Humans were used for studies that are base of this research.

CONSENT FOR PUBLICATION

Not applicable.

CONFLICT OF INTEREST

The authors declare no conflict of interest, financial or otherwise.

ACKNOWLEDGEMENTS

This work was supported by CNPq, the National Council for Scientific and Technological Development - Brazil (Proc. n. 201221/2014-4) and also sponsored by grants from FAPEMIG and CAPES. LTC is also thankful for the grants supported by FAPERJ and CNPq. SV thanks to the Portuguese Foundation for Science & Technology (FCT), through IDMEC, under LAETA, project UID/EMS/50022/2013 and Program Investigador FCT (IF/00653/2012).

REFERENCES

- [1] Leemans, C. R., Braakhuis, B. J. M., Brakenhoff, R. H. The molecular biology of head and neck cancer. *Nat Rev Cancer*, **2011**, 11(1): 9-22.
- [2] Stewart, B. W., Wild, C.P. *World Cancer Report 2014*. Lyon: IARC; **2014**.
- [3] Instituto Nacional de Cancer Jose Alencar Gomes da Silva. Laringe <http://www2.inca.gov.br/wps/wcm/connect/tiposdecancer/site/home/laringe> (Accessed Jan 20, 2017).
- [4] Syrjänen, S. The role of human papillomavirus infection in head and neck cancers. *Annals of Oncology*, **2010**, 21(suppl_7): vii243-vii245.
- [5] Silveira, N. J., Varuzza, L., Machado-Lima, A., Lauretto, M. S., Pinheiro, D. G., Rodrigues, R. V., Severino, P., Nobrega, F. G., Silva, W. A., de B Pereira, C. A., Tajara, E. H. Searching for molecular markers in head and neck squamous cell carcinomas (HNSCC) by statistical and bioinformatic analysis of larynx-derived SAGE libraries. *BMC Medical Genomics*, **2008**, 1(1): 56.
- [6] Kimple, A. J., Torres, A. D., Yang, R. Z., Kimple, R. J. HPV-Associated Head and Neck Cancer: Molecular and Nano-Scale Markers for Prognosis and Therapeutic Stratification. *Sensors (Basel, Switzerland)*, **2012**, 12(4): 5159-5169.
- [7] Wilken, R., Veen, M. S., Wang, M. B., Srivatsan, E. S. Curcumin: A review of anti-cancer properties and therapeutic activity in head and neck squamous cell carcinoma. *Molecular Cancer*, **2011**, 10: 12-12.
- [8] Cohen, E. E. W., Lingen, M. W., Zhu, B., Zhu, H., Straza, M. W., Pierce, C., Martin, L. E., Rosner, M. R. Protein Kinase C ζ Mediates Epidermal Growth Factor-Induced Growth of Head and Neck Tumor Cells by Regulating Mitogen-Activated Protein Kinase. *Cancer Research*, **2006**, 66(12): 6296-6303.
- [9] Chang, J. T., Lu, Y. C., Chen, Y. J., Tseng, C. P., Chen, Y. L., Fang, C. W., Cheng, A. J. hTERT phosphorylation by PKC is essential for telomerase holoprotein integrity and enzyme activity in head neck cancer cells. *Br J Cancer*, **2006**, 94(6): 870-878.
- [10] Waczuk, E. P., Kamdem, J. P., Abolaji, A. O., Meinerz, D. F., Caeran Bueno, D., do Nascimento Gonzaga, T. K. S., do Canto Dorow, T. S., Boligon, A. A., Athayde, M. L., da Rocha, J. B. T., Avila, D. S. Euphorbia tirucalli aqueous extract induces cytotoxicity, genotoxicity and changes in antioxidant gene expression in human leukocytes. *Toxicology Research*, **2015**, 4(3): 739-748.
- [11] Silva, A. C. P., Faria, D. E. P. d., Borges, N. B. d. E. S., Souza, I. A. d., Peters, V. M., Guerra, M. d. O. Toxicological screening of Euphorbia tirucalli L.: Developmental toxicity studies in rats. *Journal of Ethnopharmacology*, **2007**, 110(1): 154-159.
- [12] Dutra, R. C., Claudino, R. F., Bento, A. F., Marcon, R., Schmidt, É. C., Bouzon, Z. L., Pianowski, L. F., Calixto, J. B. Preventive and Therapeutic Euphol Treatment Attenuates Experimental Colitis in Mice. *PLoS ONE*, **2011**, 6(11): e27122.

- [13] de Melo, J. G., Santos, A. G., de Amorim, E. L. C., Nascimento, S. C. d., de Albuquerque, U. P. Medicinal Plants Used as Antitumor Agents in Brazil: An Ethnobotanical Approach. *Evidence-Based Complementary and Alternative Medicine*, **2011**, 2011: 14.
- [14] Choene, M., Motadi, L. Validation of the antiproliferative effects of Euphorbia tirucalli extracts in breast cancer cell lines. *Molecular Biology*, **2016**, 50(1): 98-110.
- [15] Munro, B., Vuong, Q. V., Chalmers, A. C., Goldsmith, C. D., Bowyer, M. C., Scarlett, C. J. Phytochemical, Antioxidant and Anti-Cancer Properties of Euphorbia tirucalli Methanolic and Aqueous Extracts. *Antioxidants*, **2015**, 4(4): 647-661.
- [16] Valadares, M. C., Carrucha, S. G., Accorsi, W., Queiroz, M. L. S. Euphorbia tirucalli L. modulates myelopoiesis and enhances the resistance of tumour-bearing mice. *International Immunopharmacology*, **2006**, 6(2): 294-299.
- [17] Dutra, R. C., Campos, M. M., Santos, A. R. S., Calixto, J. B. Medicinal plants in Brazil: Pharmacological studies, drug discovery, challenges and perspectives. *Pharmacological Research*, **2016**, 112: 4-29.
- [18] Gupta N., V. G., Wal A., Wal P. Medicinal Value of Euphorbia tirucalli : A Review. *Systematic Reviews in Pharmacy*, **2013**, 1(1): 16-25.
- [19] Priya CL, R. K. A review o Phytochemical a Pharmacological Profile of Euphorbia Tirucalli. *Pharmacologyonline*, **2011**, 2: 384-390.
- [20] Yoshida, T., Yokoyama, K.-i., Namba, O., Okuda, T. Tannins and Related Polyphenols of Euphorbiaceae Plants. VII. Tirucallins A, B and Euphorbin F, Monomeric and Dimeric Ellagitannins from Euphorbia tirucalli L. *CHEMICAL & PHARMACEUTICAL BULLETIN*, **1991**, 39(5): 1137-1143.
- [21] Yamamoto, Y., Mizuguchi, R., Yamada, Y. Chemical constituents of cultured cells of Euphorbia tirucalli and E. millii. *Plant cell reports*, **1981**, 1(1): 29-30.
- [22] Gupta, R. K., Mahadevan, V. Chemical examination of the stems of Euphorbia tirucalli. *Indian journal of pharmacology*, **1967**, 42: 152-154.
- [23] Jahan, N., Rahman, K.U., Ali, S., Asi, M.R. Phenolic acid and favonol contents of gemmo-modified and native extracts of some indigenous medicinal plants. *Pak J Bot*, **2013**, 45(5): 1515-1519.
- [24] Kuster, R. M., Caxito, M. L. C., Sabino, K. C. C., da Costa, H. B., Tose, L. V., Romão, W., Vaz, B. G., Silva, A. G. Identification of maloyl glucans from Euphorbia tirucalli by ESI(-)-FT-ICR MS analyses. *Phytochemistry Letters*, **2015**, 12: 209-214.
- [25] Lin, S.-J., Yeh, C.-H., Yang, L.-M., Liu, P.-C., Hsu, F.-L. Phenolic Compounds from Formosan Euphorbia tirucalli. *Journal of the Chinese Chemical Society*, **2001**, 48(1): 105-108.
- [26] Geromichalos, G. D. Importance of molecular computer modeling in anticancer drug development. *Journal of BUON : official journal of the Balkan Union of Oncology*, **2007**, 12 Suppl 1: S101-118.
- [27] Saraiva, L. A., Veloso, M. P., Camps, I., da Silveira, N. J. Structural Bioinformatics Approach of Cyclin-Dependent Kinases 1 and 3 Complexed with Inhibitors. *Molecular informatics*, **2011**, 30(2-3): 219-231.
- [28] Devi, C. A. Docking study on Mycobacterium tuberculosis receptors AccD5 and PKS18 with selected phytochemicals. *IOSR Journal of Pharmacy and Biological Sciences (IOSR-JPBS)*, **2012**, 4(3): 01-04.
- [29] Xavier, M. M., Heck, G. S., de Avila, M. B., Levin, N. M., Pintro, V. O., Carvalho, N. L., Azevedo, W. F., Jr. SAnDReS a Computational Tool for Statistical Analysis of Docking Results and Development of Scoring Functions. *Combinatorial chemistry & high throughput screening*, **2016**.
- [30] Wang, R., Lai, L., Wang, S. Further development and validation of empirical scoring functions for structure-based binding affinity prediction. *Journal of Computer-Aided Molecular Design*, **2002**, 16(1): 11-26.
- [31] Kumari, R., Kumar, R., Lynn, A. g_mmpbsa—A GROMACS Tool for High-Throughput MM-PBSA Calculations. *Journal of Chemical Information and Modeling*, **2014**, 54(7): 1951-1962.
- [32] Šali, A., Blundell, T. L. Comparative Protein Modelling by Satisfaction of Spatial Restraints. *Journal of molecular biology*, **1993**, 234(3): 779-815.
- [33] The UniProt, C. The Universal Protein Resource (UniProt). *Nucleic Acids Research*, **2007**, 35(Database issue): D193-D197.
- [34] Berman, H. M., Westbrook, J., Feng, Z., Gilliland, G., Bhat, T. N., Weissig, H., Shindyalov, I. N., Bourne, P. E. The Protein Data Bank. *Nucleic Acids Research*, **2000**, 28(1): 235-242.
- [35] Altschul, S. F., Madden, T. L., Schäffer, A. A., Zhang, J., Zhang, Z., Miller, W., Lipman, D. J. Gapped BLAST and PSI-BLAST: a new generation of protein database search programs. *Nucleic Acids Research*, **1997**, 25(17): 3389-3402.
- [36] Takimura, T., Kamata, K., Fukasawa, K., Ohsawa, H., Komatani, H., Yoshizumi, T., Takahashi, I., Kotani, H., Iwasawa, Y. Structures of the PKC-[iota] kinase domain in its ATP-bound and apo forms reveal defined structures of residues 533-551 in the C-terminal tail and their roles in ATP binding. *Acta Crystallographica Section D*, **2010**, 66(5): 577-583.
- [37] Sievers, F., Wilm, A., Dineen, D., Gibson, T. J., Karplus, K., Li, W., Lopez, R., McWilliam, H., Remmert, M., Söding, J., Thompson, J. D., Higgins, D. G. Fast, scalable generation of high-quality protein multiple sequence alignments using Clustal Omega. *Molecular Systems Biology*, **2011**, 7: 539-539.
- [38] Laskowski, R. A., Macarthur, M. W., Moss, D. S., Thornton, J. M. {PROCHECK}: a program to check the stereochemical quality of protein structures. *J Appl Cryst*, **1993**, 26: 283-291.
- [39] Bolton, E. E., Wang, Y., Thiessen, P. A., Bryant, S. H. *Chapter 12 - PubChem: Integrated Platform of Small Molecules and Biological Activities*. In: *Annual Reports in Computational Chemistry*; Edited by Ralph, A.W., David, C.S.: Elsevier, **2008**.
- [40] O'Boyle, N. M., Banck, M., James, C. A., Morley, C., Vandermeersch, T., Hutchison, G. R. Open Babel: An open chemical toolbox. *Journal of Cheminformatics*, **2011**, 3(1): 33.
- [41] Sanner, M. F. Python: a programming language for software integration and development. *Journal of molecular graphics & modeling*, **1999**, 17(1): 57-61.
- [42] Trott, O., Olson, A. J. AutoDock Vina: improving the speed and accuracy of docking with a new scoring function, efficient optimization and multithreading. *Journal of computational chemistry*, **2010**, 31(2): 455-461.
- [43] Jorgensen, W., Chandrasekhar, J., Madura, J., Impey, R., Klein, M. Comparison of simple potential functions for simulating liquid water. *The Journal of Chemical Physics*, **1983**, 79(2): 926-935.
- [44] Wang, J., Wolf, R. M., Caldwell, J. W., Kollman, P. A., Case, D. A. Development and testing of a general amber force field. *Journal of Computational Chemistry*, **2004**, 25(9): 1157-1174.
- [45] Sousa da Silva, A. W., Vranken, W. F. ACPYPE - AnteChamber PYthon Parser interface. *BMC Research Notes*, **2012**, 5: 367-367.
- [46] Hess, B., Kutzner, C., van der Spoel, D., Lindahl, E. GROMACS 4: Algorithms for Highly Efficient, Load-Balanced, and Scalable Molecular Simulation. *Journal of Chemical Theory and Computation*, **2008**, 4(3): 435-447.
- [47] van der Spoel, D., Hess, B. GROMACS—the road ahead. *Wiley Interdisciplinary Reviews: Computational Molecular Science*, **2011**, 1(5): 710-715.
- [48] Pronk, S., Páll, S., Schulz, R., Larsson, P., Bjelkmar, P., Apostolov, R., Shirts, M. R., Smith, J. C., Kasson, P. M., van der Spoel, D., Hess, B., Lindahl, E. GROMACS 4.5: a high-throughput and highly parallel open source molecular simulation toolkit. *Bioinformatics*, **2013**, 29(7): 845-854.
- [49] Bussi, G., Donadio, D., Parrinello, M. Canonical sampling through velocity rescaling. *The Journal of Chemical Physics*, **2007**, 126(1): 014101.
- [50] Parrinello, M., Rahman, A. Polymorphic transitions in single crystals: A new molecular dynamics method. *Journal of Applied Physics*, **1981**, 52(12): 7182-7190.
- [51] Essmann, U., Perera, L., Berkowitz, M., Darden, T., Lee, H., Pedersen, L. A smooth particle mesh Ewald method. *The Journal of Chemical Physics*, **1995**, 103(19): 8577-8593.
- [52] Hess, B., Bekker, H., Berendsen, H., Fraaije, J. LINCS: A linear constraint solver for molecular simulations. *J Comput Chem*, **1997**, 18(12): 1463-1472.
- [53] Miyamoto, S., Kollman, P. Settle: An analytical version of the SHAKE and RATTLE algorithm for rigid water models. *J Comput Chem*, **1992**, 13(8): 952-962.
- [54] Baker, N. A., Sept, D., Joseph, S., Holst, M. J., McCammon, J. A. Electrostatics of nanosystems: Application to microtubules and the ribosome. *Proceedings of the National Academy of Sciences*, **2001**, 98(18): 10037-10041.

- [55] Laskowski, R. A., Swindells, M. B. LigPlot+: Multiple Ligand-Protein Interaction Diagrams for Drug Discovery. *Journal of Chemical Information and Modeling*, **2011**, 51(10): 2778-2786.
- [56] Lagorce, D., Sperandio, O., Baell, J. B., Miteva, M. A., Villoutreix, B. O. FAF-Drugs3: a web server for compound property calculation and chemical library design. *Nucleic Acids Research*, **2015**, 43(Web Server issue): W200-W207.
- [57] DeLano, W. L. The PyMOL Molecular Graphics System, Version 1.8. In., 1.8 edn: Schrodinger, LLC; 2015.
- [58] Chung, S. Y., Subbiah, S. How similar must a template protein be for homology modeling by side-chain packing methods? *Pacific Symposium on Biocomputing Pacific Symposium on Biocomputing*, **1996**: 126-141.
- [59] Chen, C.-L., Chen, Y.-P., Lin, M.-W., Huang, Y.-B., Chang, F.-R., Duh, T.-H., Wu, D.-C., Wu, W.-C., Kao, Y.-C., Yang, P.-H. Euphol from *Euphorbia tirucalli* Negatively Modulates TGF- β Responsiveness via TGF- β Receptor Segregation inside Membrane Rafts. *PLOS ONE*, **2015**, 10(10): e0140249.
- [60] May, P., Quirin, K.W. Supercritical Marigold Flower CO₂ -Extract - Evergreen in Evidence Based Cosmetic Application. *Cosmetic Science Technology*, **2014**, 1: 19-25.
- [61] Passos, G. F., Medeiros, R., Marcon, R., Nascimento, A. F. Z., Calixto, J. B., Pianowski, L. F. The role of PKC/ERK1/2 signaling in the anti-inflammatory effect of tetracyclic triterpene euphol on TPA-induced skin inflammation in mice. *European Journal of Pharmacology*, **2013**, 698(1-3): 413-420.
- [62] Sathya, S., Sudhagar, S., Sarathkumar, B., Lakshmi, B. S. EGFR inhibition by pentacyclic triterpenes exhibit cell cycle and growth arrest in breast cancer cells. *Life sciences*, **2014**, 95(1): 53-62.
- [63] Lipinski, C. A., Lombardo, F., Dominy, B. W., Feeney, P. J. Experimental and computational approaches to estimate solubility and permeability in drug discovery and development settings1. *Advanced Drug Delivery Reviews*, **2001**, 46(1-3): 3-26.

DISCLAIMER: The above article has been published in Epub (ahead of print) on the basis of the materials provided by the author. The Editorial Department reserves the right to make minor modifications for further improvement of the manuscript.